Bulletin of Environment, Pharmacology and Life Sciences
Bull. Env. Pharmacol. Life Sci., Spl Issue [1] January 2023 : 109-116

Online ISSN 2277-1808
Journal's URL:http://www.bepls.com
CODEN: BEPLAD

ORIGINAL ARTICLE **OPEN ACCESS**

Aspergillus eucalypticola SLF1 mediated TiO_2 nanosphere for Methylene Blue dye degradation

Avinash Ashok Survase[a], Shivangi Shivraj Kanase[abc*]
[a]*Rayat Institute of Research and Development, Satara 415 001, Maharashtra, INDIA*
[b]*Department of Microbiology, Yashavantrao Chavan Institute of Science, Satara, 415 001, Maharashtra,INDIA*
[*c]*P. G. Department of Microbiology, Yashavantrao Chavan Institute of Science, Satara, 415 001, Maharashtra, INDIA*
Corresponding Author
shivangikanase7@gmail.com (Dr. Ms. S. S. Kanase)

ABSTRACT:
Biosynthesis of TiO_2 nanoparticles (NPs) was achieved by using an isolated fungus Aspergillus eucalypticola SLF1 from lonar lake soil ecosystem. A simple, facile, eco-friendly and cheaper approach has been used for the green synthesis. TiO_2 NPs formation was monitored by visual observation, UV-Vis spectroscopy, Fourier transform infrared spectroscopy (FTIR), X-ray diffraction (XRD), and Scanning electron microscopy (SEM) studies. Visual observation showed white precipitate formation within 72 h at 37 ^{0}C, 140 rpm. UV-Vis spectroscopy showed maximum absorbance at 214 nm. FTIR spectra revealed presence of functional groups indicating involvement of biomolecules in capping process. XRD studies showed peaks at 25.19, 38.53, 48.04 and 53.86 respectively indicates pure anatase tetragonal crystal form of TiO_2. SEM revealed spherical shape and size of TiO_2 NPs ranging from 11 nm to 45 nm. EDAX results showed elemental composition of TiO_2 contain titanium 84.18% and 15.82% of oxygen. Mycogenic synthesized TiO_2 NPs showed excellent photocatalytic application for methylene blue dye degradation (91%) within 30 min under sunlight irradiation.
Keywords: *Green synthesis, TiO_2 nanosphere, Aspergillus eucalypticola SLF1, Biophysical haracterization, Photocatalytic activity*

Received 02.10.2022 Revised 23.11.2022 Accepted 10.12.2022

INTRODUCTION

The rapid industrialization of the world released large amounts of wastewater effluents, leading to face problems with aquatic contamination through azo, diazo,synthetic dyes and medications, which are widely contaminating potable water [1, 2]. The amount of water pollutants rise day by dye [3]. Long time persistance of these non degradable pollutants creates hazardous effect on environment [4]. Methylene blue (MB), malachite green (MG), rhodamine B (Rh. B.) and many other various textile dye sources are discharged frequently in potable water [5, 6].

One of the major sources of textile industry pollutant is MB dye. MB which is mutagenic and carcinogenic dye damaging to both human life and the aquatic environment. To eliminate toxic water pollution and turn it into usable water, is a challanging task to researchers. A variety of physical, chemical and biological approaches have been developed to break down dyes and turn contaminated water into useful water. photocatalytic degradation, using NPs is a significant advancement in textile dye remediation field [4].

The oxidation-reduction reaction having significant role in remediation. Sunlight driven NPs activated advance oxidation methodoly is new emerging photocatalytic approach for degradation of dyes into CO_2 and H_2O [7]. NPs mediated Photocatalytic dye remediation is simple, cost effective, less time consuming and low temperature requirng approach [8, 9].The selection of ideal photocatalyst on the basis of bandgap, large specific area, low-cost production, high oxidizing and reducing property. Metal oxide and metal oxide composite with large specific surface area materials attracted great intreast due to its effective photocatalytic degradation using advanced oxidation process . TiO_2, Fe_2O_3, V_2O_5, ZnO, TiO_2-rGO, WO_3-rGO, Fe_2O_3, WO_3 are such promising candidates having wide surface to volume ratio, working at low temperature, excellent stability, and favorable semiconductor nature [10].

In recent years TiO_2 material has been multifunctional use in the area of solar cells [11], sensor [12], antimicrobial activities, photocatalyst [13], fertilizer [14], plastics [15]. Several successful physical and chemical methods are broadly used for synthesis of TiO_2 NPs, which include sol-gel method [16],

hydrothermal method [17], and sonochemical method [18]. These approaches offers some drawback such as consumption of energy to maintain high pressure and temperature during synthesis of NPs and formation various toxic byproducts [19], to overcome these issues today need to introduce another facile alternative mathod for the synthesis NPs. Biological synthesis of NPs using microorganism has been of special interest to researcher because of easy handling procedure ecofriendly decomposition and easier downstream processing [20]. Another key aspect of fungus is they extracellularly secrete large amount of enzymes for reduce metal salt to nanscale diameter. Microorganism anionic electro potential enables to attract the cations and act as a trigger for biosynthesis of metal oxide NPs[14].

TiO_2 has received wide attention due to its promising properties like appropriate bandgap (~3.2 eV), large surface area, and active photocatalytic property. TiO_2 exists in three different crystalline forms namely anatase, rutile and brookite. The anatase phase is more stable than the rutile phase at temperatures ranging between 325 and 750 °C [21]. The different phase stability in TiO_2 NPs is related to their physical environment and the interaction between TiO_2 and H_2O [22]. Out of three polymorph structures, anatase phase TiO_2 increases e^--h^+ splitting and decrease e^--h^+ recombination lead to cause enhancement of photocatalytic activity.

In present research, we sucessfully developed biologically inspired experimental protocol for synthesis of stable TiO_2 nanospheres by using lonar lake isolated fungi *Aspergillus eucalypticola SLF1*. Green synthesis is an environmentally safe, cost-effective, nontoxic, and biocompatible approach. Ultraviolet spectroscopy show maximum TiO_2 Optical absorption in ultraviolet region. The sharp intense peak of XRD reveal anatase crystal phase TiO_2. Monodisperse morphology is observed under SEM. Sunlight driven TiO_2 NPs show 91% photocatalytic degradation of methylene blue dye within 30 min.

MATERIAL AND METHODS

Chemicals and media

Titanium chloride ($TiCl_3$-purity 99%), Sabouraud dextrose broth, agar-agar was procured from Hi-Media laboratories Pvt. Ltd., India. Milli-Q-water used for prepared all aqueous solutions. All chemicals were analytical grade. The textile dye methylene blue dye was procured from the from textile industry, solapur.

Isolation and Identification of fungi

For the experiment soil sample was collected from Lonar lake, Buldhana, Maharashtra, India. Soil sample air dried and use for isolation of fungi. For isolation fungi soil sample was serially diluted up to 10^{-5} and spread on sabouraud dextrose agar, as selective media for fungi. Incubate all plates at 37 ^{0}C for 72 h in BOD incubator.Isolated fungi were identified by use phenotypic characterization and phylogenetic analysis. Maintain stock culture at 4^{0}C in refrigerator. Use an actively growing culture for nanoparticle synthesis.

Synthesis of TiO_2 nanoparticle using fungi.

TiO_2 NPs were synthesized using biological method. For the synthesis TiO_2 NPs *Aspergillus eucalypticolaSLF1* was grown in 250 ml Erlenmeyer flask containing 100ml Sabouraud dextrose broth having pH 5.8. The culture was kept on rotator shaker at 140 rpm at 37 ^{0}C for 72 h, for development fungal mycelia. Mycelia were separated out by Whatman filter paper no.1 followed by thrice washing with Milli-Q-water. Harvested mycelia (15gm fresh biomass) were inoculated in 100ml Milli-Q-water and incubated for 62h at 37^{0}C on rotatory shaker 140rpm.

Collected cell free extract containing fungus secreted extracellular biomolecules which was mixed with precursor metal salt titanium chloride at 10^{-3}M concentration and incubated for 48 h at 37 ^{0}C at 140 rpm for bio-transformed TiO_2 NPs [14].

Characterization of TiO_2 nanoparticles

The excitation spectra of bio-transformed TiO_2 NPs were monitored by using double beam UV-Visible spectrophotometer (Systronics AU-270-I). The dried powder was mixed with potassium bromide for prepared fine pellet and recorded spectrum using single beam spectrophotometer (FTIR-7600 Lambda Scientific Spectrum Spectrometry) within range 400-4000 cm^{-1} to identify involvement of biomolecules in TiO_2 nanoparticle synthesis. Crystallographic structure and phage of NPs was monitored by using powder XRD analysis on (Rigaku 600 Miniflex benchtop x-ray diffractmeter) having Cu Kα radiation (λ=1.54A^0) in the range (2Θ) of 20^0-80^0 at 40kV/40mA. The surface morphology of TiO_2 nanoparticle was study by scanning electron microscopy (SEM, Hitachi S-4800). The photocatalytic activity of TiO_2 NPs were investigated by using a fluorescence spectrophotometer (Varian Cary Eclipse) and double beam UV-Visible spectrophotometer (Systronics AU-270-I).

Photocatalytic activity of biosynthesized TiO_2 NPs in the degradation of Methylene Blue dye

In order to study the photocatalytic activity of Methylene Blue dye, 100 ml of 10 ppm freshly prepared dye solution was mixed with 1 mg of biosynthesized TiO2 photocatalyst. The 10 ppm dye solution without TiO_2 NPs was kept as a control. The dye solution with catalyst i.e. test solution was under sunlight.

From the mixture of solution (5 ml), aliquots were withdrawn from the test solution every 10 min time interval and centrifuged (10000 rpm, 10 min). The absorption spectrum of the supernatant was recorded using a UV-Vis spectrophotometer. The dye degradation percentage was calculated as

$$Efficiency\ of\ degradation\ (\%) = \frac{(C_0 - C_t)}{C_0} \times 100 \qquad \text{.....(1)}$$

Where, C_0 is initial absorbance of dye solution without catalyst, and C_t is the absorbance of the dye with catalyst at time t, The rate constant of first order kinetic reaction 'k_{app}' was calculated by using the equation [23],

$$\ln\left(\frac{C_t}{C_0}\right) = -k_{app}t \qquad \text{.....(2)}$$

RESULTS AND DISCUSSION

UV-Visible Spectroscopy

UV-Visible spectroscopy is an useful technique to study the kinetic of formation of TiO_2 NPs, electronic transition occurs due to absorption of UV-Vis capable to generating electron from empty orbital. Visual observation showed white precipitate formation within 48 h at 37 ^{0}C, 140 rpm, based on Fig. 1 show that TiO_2 NPs showed absorption peak at 214 nm. TiO_2 can absorb ultra-violet light having wavelength less than 387 nm, The strong absorption at range 200 nm – 340 nm indicates the formation of the TiO_2 NPs [24], but the exact position may changes due to various factors such as size and shape of NPs [25].

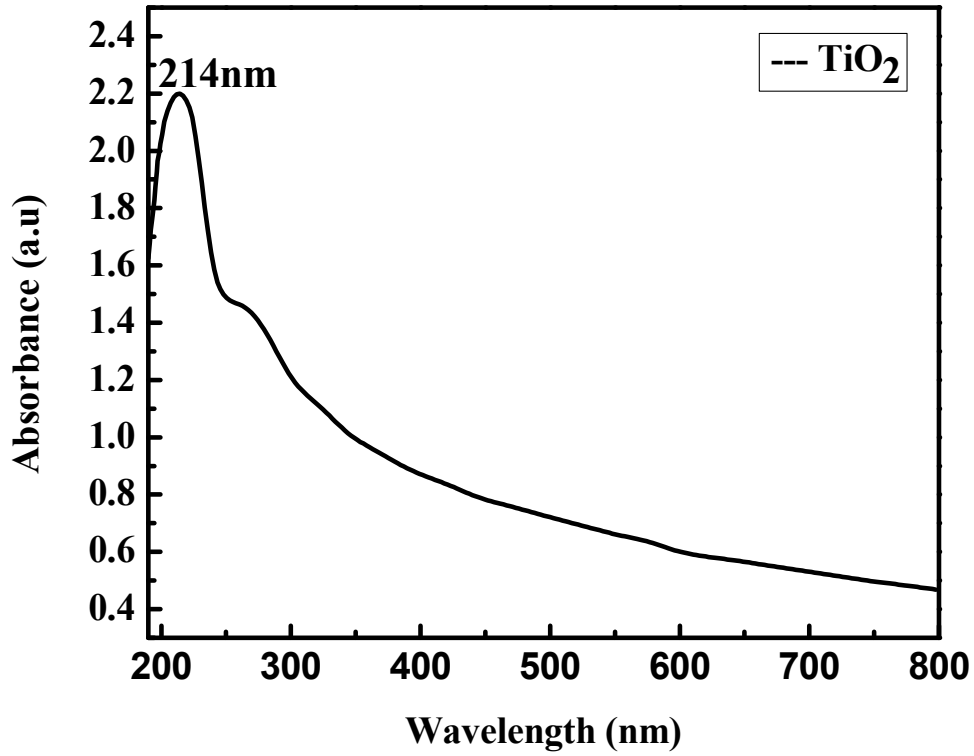

Fig. 1. UV-Visible spectra of TiO_2 Nanoparticles

FTIR

FTIR spectra revealed presence of functional groups indicating involvement of biomolecules in capping process, it showed supporting information for confirmation of TiO_2 NPs. The FTIR spectrum cell free extract mediated TiO_2 NPs clearly showed in Fig. 2. shows six distinct peaks at 3427 cm^{-1}, 2924 cm^{-1}, 1652 cm^{-1}, 1395 cm^{-1}, 1020 cm^{-1} and 684 cm^{-1}.The broadest peak at 3427 cm^{-1} may be attributed due to N-H stretching frequency arising from the peptide linkage present in the protein of the biosynthesis of *Aspergillus eucalypticola SLF1* using TiO_2. The band at 2924 cm^{-1} could be due to capped NPs confirms the bound carboxylic groups with Ti-O-Ti [26]. The peak at 1652 cm^{-1} indicates characteristics of amide stretching and N-H bending. The peak at 1395 cm^{-1} related to Ti-O modes. The peak at 1020 cm^{-1} shows presence of some C-O ether linkage.The peak observed at 684 cm^{-1} is due to the vibration of the Ti-O-O bond [27]

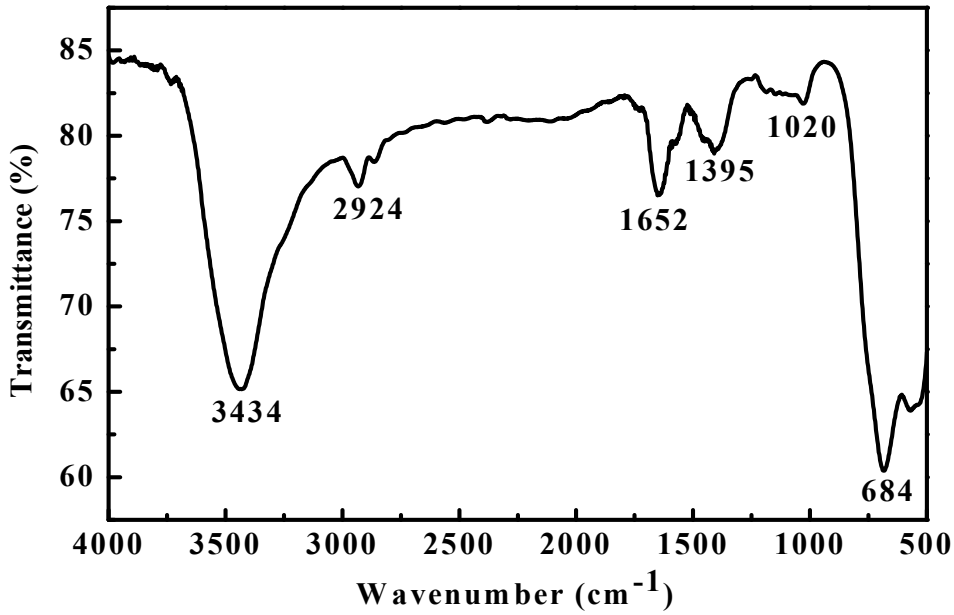

Fig. 2. FTIR spectra of TiO_2 Nanoparticles

XRD

XRD use to analyze crystalline nature of TiO_2 NPs shown in Fig. 3. The average crystallite size of TiO_2 NPs was calculated from XRD pattern using Debye Scherrer's equation [28]:

$D = K\lambda / \beta \cos\theta$ ……(3)

Where, D is average mean diameter of NPs, K is the crystalline shape constant (K=0.89), λ is the wavelength of X-ray, θ is the Braggs diffraction angle and β is the angular full width at half maxima (FWHM) of XRD peaks recorded at diffraction angle 2θ. The average crystallite size of TiO_2 NPs calculated using Debye Scherrer's equation is 33.89 nm.

The XRD pattern recorded distinct Braggs peaks observed over the range 2θ values from 20^0 to 80^0 at 25.28^0, 37.12^0, 37.80^0, 38.71^0, 47.97^0, 53.81^0, 55.10^0, 62.67^0, 68.57^0, 70.49^0, 75.10^0 were corresponds to the miller indices (hkl) plane values (101), (103), (004), (112), (200), (105), (214), (204), (116), (220) and (215) respectively. The intense peak 2θ at 25.28^0 matched the (101), confirmed that biosynthesized TiO_2 NPs in anatase crystallographic phase, broad width of the peaks clearly showed the smaller size of NPs [29]

XRD results match with tetragonal anatase phase of crystalline TiO2 NPs with space group I41/amd (141) and lattice parameters were a=b=3.785 A^0, c=9.5139 A^0 with JCPDS card No. 21-1272.

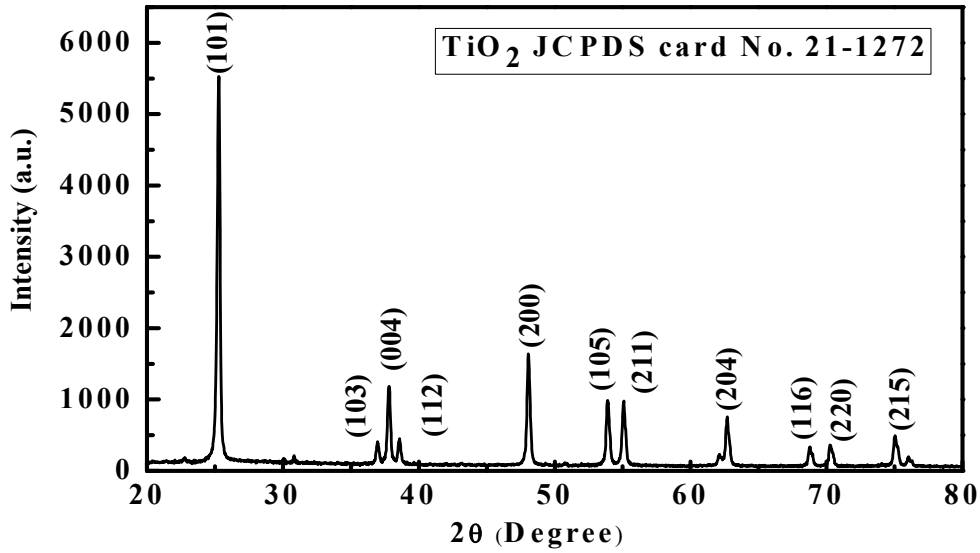

Fig. 3. XRD spectra of TiO_2 Nanoparticles

SEM& EDX

The SEM technique was used to determine surface morphology of TiO_2 NPs. The SEM image of the *Aspergillus eucalypticola SLF1* synthesized TiO_2 NPs shown spherical in shape Fig. 4 (a). The observed micrograph shows monodisperced nanospheres of TiO_2 NPs having size less than 50 nm.

The EDS spectrum of biotransformed product analyzed by SEM equipped with energy dispersive X-ray spectroscopy (SEM-EDX). Fig. 4 (b) shows the highest peak intensity of titanium metal at 4.6keV (84.18 %) and low intensity of peak of oxygen (15.82) due to dissociation of precursor compounds represents the conformation of purity of TiO_2 NPs.

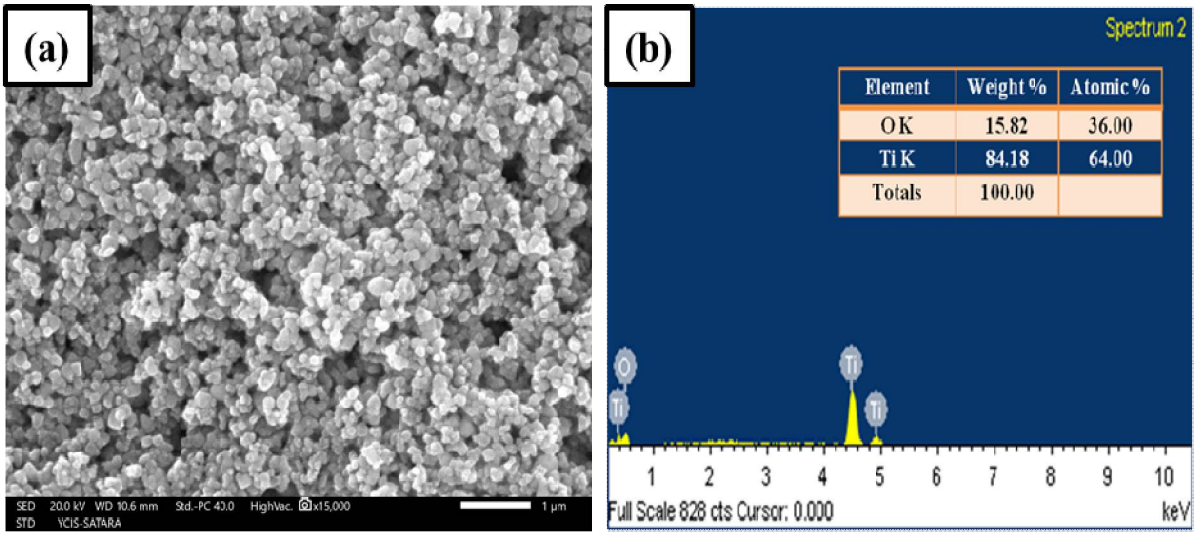

Fig. 4. a) Scanning electron microscopy and b) Elemental analysis of TiO_2 nanoparticles

3.5. Photocatalytic activity of TiO_2 NPs.

In present work, we have studied the photocatalytic performance of fungus-mediated TiO_2 NPs. Depending on the photocatalytic activity working principle, different NPs such as Fe, Ag, Au, Se, Cu, and ZnO are used for dye degradation. The Methylene Blue degradation mechanism using TiO_2 catalyst is explained below**.**

In this degradation reaction mechanism, when a photon of energy comparable with the band gap of TiO_2 impinge on the catalyst it generates electron and hole at conduction and valence band respectively. The holes in valence band produces OH^- radicals due to oxidation reaction with water molecules present on the catalyst surface, while electrons in the conduction band produce superoxide radicals O_2^-. Further this OH^- radical reacts with organic matter in the dye which produces an intermediate product and this intermediate product reacts with superoxide ion to produce peroxide or hydrogen peroxide which leads to the formation of water molecules [30].

The photocatalytic potential of biosynthesized TiO_2 NPs for degradation of Methylene Blue dye was investigated under continuous irradiation of sunlight. It was monitored using a UV-visible spectroscopy shown in Fig. 5. (A). The observed characteristic wavelength of Methylene Blue dye is 668 nm. An addition of TiO_2 NPs into Methylene Blue dye mixture turns gradual degradation of dye and colorless solution observed within a short interval (30 min). A progressive reduction in peak intensity maximum at 668 nm was detected which reveals 91% degradation shown in Fig. 5. (B). The Surface Plasmon Resonance (SPR) peak for TiO_2 NPs was not observed in UV-Visible spectrum during the catalytic study. From the plot of ln (C_t/C_0) vs time, the rate constant (K_{app}) value was calculated and it is found to be 0.03656 min^{-1} shown in Fig. 5. (C). This indicates the reduction reaction follows pseudo-first-order kinetics and good linear correlation between ln (C_t/C_0) Vs time. Fig. 5. (D). show photographs of before methylene blue dye remediation and after dye remediation.

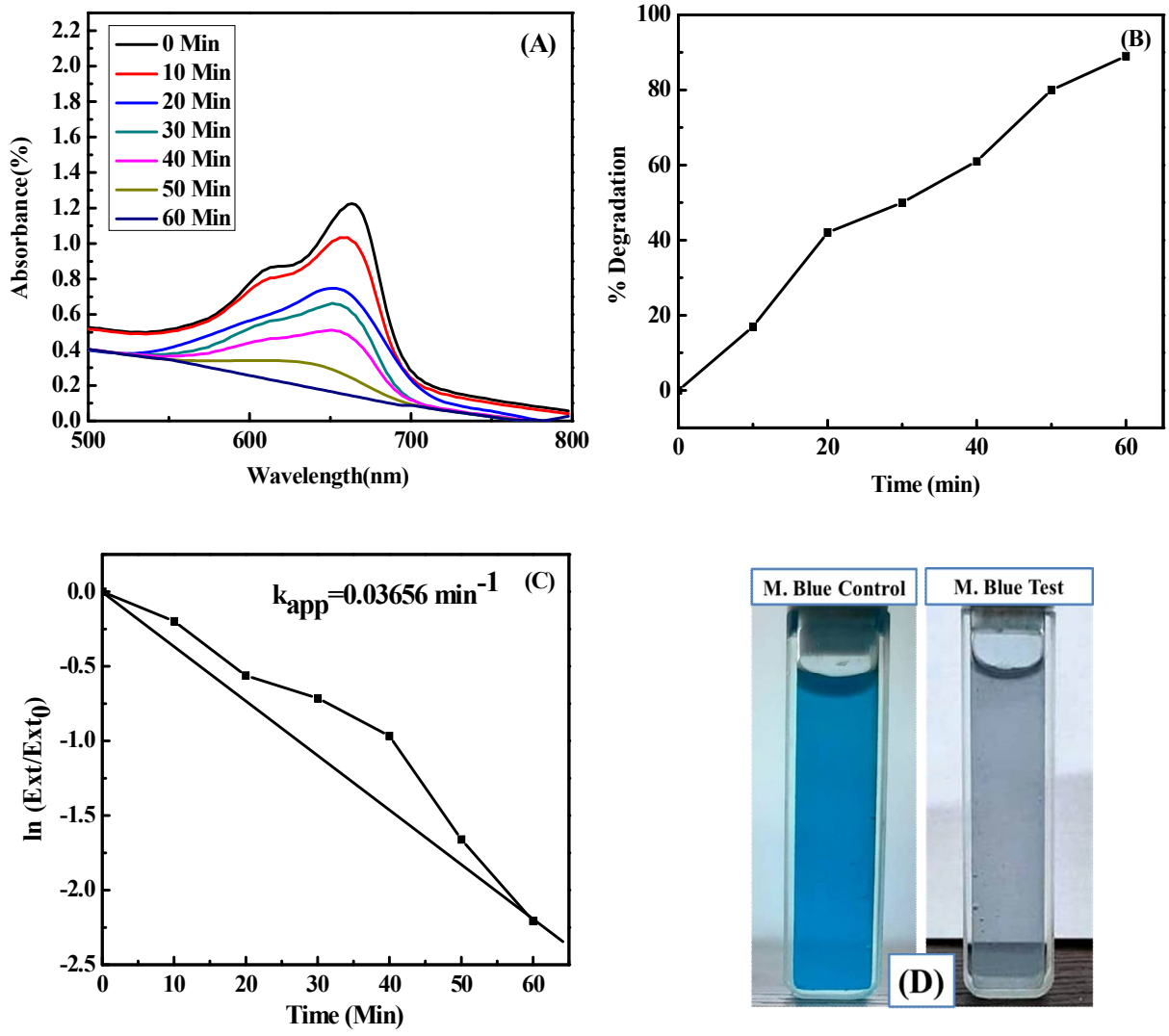

Fig. 5. (A) UV–Visible Absorption spectra of Methylene Blue dye using rGO NMs at various time interval
(B) Degradation % of Methylene Blue dye with time in presence of rGO material.
(C)ln(Ct/Co) verses degradation time plot for finding the reaction rate constant (k_{app}).
(D) Show photographs of Methylene Blue before and after degradation

CONCLUSION

In conclusion, we have reported a facile eco-friendly inexpensive rapid method for synthesis of TiO_2 NPs using Lonar lake isolated fungus *Aspergillus eucalypticolaSLF1* reported first time. The biosynthesis TiO_2 NPs were characterized by using UV-Vis, XRD, FTIR, SEM and EDX which revealed spherical, anatase, tetragonal structure of TiO_2 NPs having average size 33.89 nm. Biological prepared TiO_2 NPs show excellent photocatalytic activity of methylene blue dye 91% within 30 min under sunlight irridiation. Overall, this smart sustainable eco-friendly material can be used as potential candidate for industrial waste water effluents treatment

DECLARATION OF COMPETING INTERESTS

The authors declare that they have no known competing financial interests or personal relationships that could have appeared to influence the work reported in this paper.

ACKNOWLEDGEMENT

The author Mr. Avinash A. Survase would like to thanks the CSIR-UGC, New Delhi, India for the financial support under the Junior Research Fellowship-2019. All authors are also thankful to Rayat Institute of

Research and Development, Satara and Yashavantrao Chavan Institute of Science, Satara for providing laboratory facilities.

REFERENCES

1. Hunge, Y. M., Yadav, A. A., Dhodamani, A. G., Suzuki, N., Terashima, C., Fujishima, A., &Mathe, V. L. (2020). Enhanced photocatalytic performance of ultrasound treated GO/TiO2 composite for photocatalytic degradation of salicylic acid under sunlight illumination. Ultrasonicssonochemistry, 61, 104849.
2. Yadav, A. A., Hunge, Y. M., & Kang, S. W. (2021). Porous nanoplate-like tungsten trioxide/reduced graphene oxide catalyst for sonocatalytic degradation and photocatalytic hydrogen production. Surfaces and Interfaces, 24, 101075.
3. Shanmugam, M., Alsalme, A., Alghamdi, A., &Jayavel, R. (2015). Enhanced photocatalytic performance of the graphene-V2O5 nanocomposite in the degradation of methylene blue dye under direct sunlight. ACS applied materials & interfaces, 7(27), 14905-14911.
4. Hunge, Y. M., Yadav, A. A., Khan, S., Takagi, K., Suzuki, N., Teshima, K., ...&Fujishima, A. (2021). Photocatalytic degradation of bisphenolA using titanium dioxide@ nanodiamond composites under UV light illumination. Journal of Colloid and Interface Science, 582, 1058-1066.
5. Jayaraj, S. K., Sadishkumar, V., Arun, T., &Thangadurai, P. (2018). Enhanced photocatalytic activity of V2O5 nanorods for the photodegradation of organic dyes: a detailed understanding of the mechanism and their antibacterial activity. Materials Science in Semiconductor Processing, 85, 122-133.
6. Hunge, Y. M., Yadav, A. A., Kang, S. W., & Kim, H. (2022). Photocatalytic degradation of tetracycline antibiotics using hydrothermally synthesized two-dimensional molybdenum disulfide/titanium dioxide composites. Journal of Colloid and Interface Science, 606, 454-463.
7. Khan, M. M., Pradhan, D., &Sohn, Y. (Eds.). (2017). Nanocomposites for visible light-induced photocatalysis (Vol. 101). Springer International Publishing.
8. Yadav, A. A., Kang, S. W., &Hunge, Y. M. (2021). Photocatalytic degradation of Rhodamine B using graphitic carbon nitride photocatalyst. Journal of Materials Science: Materials in Electronics, 32(11), 15577-15585.
9. Hunge, Y. M., Uchida, A., Tominaga, Y., Fujii, Y., Yadav, A. A., Kang, S. W., ...&Terashima, C. (2021). Visible light-assisted photocatalysis using spherical-shaped bivo4 photocatalyst. Catalysts, 11(4), 460.
10. Hunge, Y. M., Yadav, A. A., &Mathe, V. L. (2018). Ultrasound assisted synthesis of WO3-ZnO nanocomposites for brilliant blue dye degradation. *Ultrasonicssonochemistry*, *45*, 116-122.
11. Malevu, T. D., Mwankemwa, B. S., Motloung, S. V., Tshabalala, K. G., &Ocaya, R. O. (2019). Effect of annealing temperature on nano-crystalline TiO2 for solar cell applications. *Physica E: Low-dimensional Systems and Nanostructures*, *106*, 127-132.
12. Grochowska, K., Ryl, J., Karczewski, J., Śliwiński, G., Cenian, A., &Siuzdak, K. (2019). Non-enzymatic flexible glucose sensing platform based on nanostructured TiO2–Au composite. *Journal of Electroanalytical Chemistry*, *837*, 230-239.
13. Hassan, S. M., Ahmed, A. I., &Mannaa, M. A. (2018). Structural, photocatalytic, biological and catalytic properties of SnO2/TiO2 nanoparticles. *Ceramics International*, *44*(6), 6201-6211.
14. Raliya, R., Biswas, P., & Tarafdar, J. C. (2015). TiO2 nanoparticle biosynthesis and its physiological effect on mung bean (Vigna radiata L.). Biotechnol Rep 5: 22–26. *Link: https://goo. gl/ZgbMBZ*.
15. Z.N. Jameel, A.J. Haider, S.Y. Taha, S. Gangopadhyay., S. Bok. (2016), Evaluation of Hybrid Sol-gel Incorporated with Nanoparticles as Nano Paint, Technologies and Materials for Renewable Energy, Environment and Sustainability AIP Conf. Proc. 1758, 020001-1–020001-14
16. Dubey, R. S. (2018). Temperature-dependent phase transformation of TiO2 nanoparticles synthesized by sol-gel method. *Materials Letters*, *215*, 312-317.
17. Santhi, S. characterization of TiO2 nanorods by hydrothermal method with different pH conditions and their photocatalytic activity. *Appl. Surf. Sci*, (500).
18. Wattanawikkam, C., &Pecharapa, W. (2020). Structural studies and photocatalytic properties of Mn and Zn co-doping on TiO2 prepared by single step sonochemical method. *Radiation Physics and Chemistry*, *171*, 108714.
19. Giannousi, K.; Avramidis, I.; Dendrinou-Samara, C. (2013). *Synthesis, characterization and evaluation of copper based nanoparticles as agrochemicals against Phytophthorainfestans. RSC Advances, 3(44), 21743–* . doi:10.1039/C3RA42118J
20. Velusamy, P., Kumar, G. V., Jeyanthi, V., Das, J., &Pachaiappan, R. (2016). Bio-inspired green nanoparticles: synthesis, mechanism, and antibacterial application. *Toxicological research*, *32*(2), 95-102.
21. Banfield, J. (1998). Thermodynamic analysis of phase stability of nanocrystalline titania. *Journal of Materials Chemistry*, *8*(9), 2073-2076.
22. Koparde, V. N., & Cummings, P. T. (2008). Phase transformations during sintering of titania nanoparticles. *ACS nano*, *2*(8), 1620-1624.
23. Torane, A. P., Ubale, A. B., Kanade, K. G., &Pagare, P. K. (2021). Photocatalytic dye degradation study of TiO2 material. *Materials Today: Proceedings*, *43*, 2738-2741.
24. Naik, G. K., Mishra, P. M., &Parida, K. (2013). Green synthesis of Au/TiO2 for effective dye degradation in aqueous system. *Chemical Engineering Journal*, *229*, 492-497.
25. Mohamed, M. B., Volkov, V., Link, S., & El-Sayed, M. A. (2000). Thelightning'goldnanorods: fluorescence enhancement of over a million compared to the gold metal. *Chemical Physics Letters*, *317*(6), 517-523.

26. Rajakumar, G., Rahuman, A. A., Roopan, S. M., Khanna, V. G., Elango, G., Kamaraj, C., &Velayutham, K. (2012). Molecular and Biomolecular Spectroscopy Fungus-mediated biosynthesis and characterization of TiO2 nanoparticles and their activity against pathogenic bacteria. *Spectrochim. Acta Part A*, *91*, 23-29.
27. Hardy, A., D'Haen, J., Van Bael, M. K., &Mullens, J. (2007). An aqueous solution–gel citratoperoxo–Ti (IV) precursor: synthesis, gelation, thermo-oxidative decomposition and oxide crystallization. *Journal of sol-gel science and technology*, *44*(1), 65-74.
28. Hargreaves, J. S. J. (2016). Some considerations related to the use of the Scherrer equation in powder X-ray diffraction as applied to heterogeneous catalysts. *Catalysis, Structure & Reactivity*, *2*(1-4), 33-37.
29. Shirke, B. S., Korake, P. V., Hankare, P. P., Bamane, S. R., &Garadkar, K. M. (2011). Synthesis and characterization of pure anatase TiO2 nanoparticles. *Journal of Materials Science: Materials in Electronics*, *22*(7), 821-824.
30. Babar, B. M., Mohite, A. A., Patil, V. L., Pawar, U. T., Kadam, L. D., Kadam, P. M., &Patil, P. S. (2021). Sol-gel prepared vanadium oxide for photocatalytic degradation of methylene blue dye. *Materials Today: Proceedings*, *43*, 2673-2677.

CITATION OF THIS ARTICLE

A. A. Survasea and S. S. Kanase: Aspergillus eucalypticola SLF1 mediated TiO2 nanosphere for Methylene Blue dye degradation, Bull. Env.Pharmacol. Life Sci., Spl Issue [1]: 2023:109-116.